Front. Mech. Eng. 2016, 11(4): 412–422
DOI 10.1007/s11465-016-0396-8

RESEARCH ARTICLE

Guizhong XIE, Dehai ZHANG, Jianming ZHANG, Fannian MENG, Wenliao DU, Xiaoyu WEN

Implementation of sinh method in integration space for boundary integrals with near singularity in potential problems

Abstract As a widely used numerical method, boundary element method (BEM) is efficient for computer aided engineering (CAE). However, boundary integrals with near singularity need to be calculated accurately and efficiently to implement BEM for CAE analysis on thin bodies successfully. In this paper, the distance in the denominator of the fundamental solution is first designed as an equivalent form using approximate expansion and the original sinh method can be revised into a new form considering the minimum distance and the approximate expansion. Second, the acquisition of the projection point by Newton-Raphson method is introduced. We acquire the nearest point between the source point and element edge by solving a cubic equation if the location of the projection point is outside the element, where boundary integrals with near singularity appear. Finally, the subtriangles of the local coordinate space are mapped into the integration space and the sinh method is applied in the integration space. The revised sinh method can be directly performed in the integration element. A verification test of our method is proposed. Results demonstrate that our method is effective for regularizing the boundary integrals with near singularity.

Keywords computer aided engineering (CAE), boundary element method (BEM), near singularity, sinh method, coordinate transformation, integration space

Received April 25, 2016; accepted May 24, 2016

Guizhong XIE, Fannian MENG, Wenliao DU (✉), Xiaoyu WEN
Mechanical and Electrical Engineering Institute, Zhengzhou University of Light Industry, Zhengzhou 450002, China
E-mail: dwenliao@zzuli.edu.cn

Dehai ZHANG (✉)
Mechanical and Electrical Engineering Institute, Zhengzhou University of Light Industry, Zhengzhou 450002, China; State Key Laboratory for Manufacturing Systems Engineering, Xi'an Jiaotong University, Xi'an 710049, China
E-mail: zhangdehai0318@163.com

Jianming ZHANG
State Key Laboratory of Advanced Design and Manufacturing for Vehicle Body, College of Mechanical and Vehicle Engineering, Hunan University, Changsha 410082, China

1 Introduction

Computer aided engineering (CAE) has been widely used in the field of airplanes, machinery, and petroleum, where it provides analytical information in the product development process in a timely manner. The quality of product can be improved and production time can be shortened significantly by implanting modern CAE techniques into the manufacturing process. Thus, the product market benefits from the CAE techniques and feedback is sent to the manufacturing factory to refine the product quality [1]. The main numerical methods used in CAE include finite element method (FEM) [2–7], boundary element method (BEM) [7–11], etc. BEM is a more promising method, which has a higher precision for flux and stress than FEM in terms of the theory for differential and integral equations [4–11]. However, another problem is encountered when BEM is used in CAE analysis on thin bodies. The problem is how to remove near singularity in boundary integrals when using BEM [9–16]. Thus, this work focuses on improving the original sinh method, to remove near singularity and compute the integrals using Gaussian quadrature directly and accurately. The goal of this paper is to improve the application of BEM in CAE analysis.

Problems need to be simulated on thin bodies and structures with features, like cracks, in many CAE analyses using BEM in industrial engineering. Appropriate treatment to remove the near singularity in the integrals is indispensable in obtaining accurate results [9–16]. The accurate and efficient evaluation of nearly singular integrals is important for implementing BEM for CAE

analysis. When the source point is close to the element in BEM and the ratio between the source point and element is very small, the integrals in this element are called nearly singular integrals. The Gaussian quadrature cannot be applied to integrals with singularity directly because of the poor computational results. The origin of near singularity comes from when the distance in the fundamental solution is close to zero. The fundamental solution tends to be infinite, and thus the standard Gaussian quadrature fails for these type of integrals. The regularization of this type of integrals to apply the standard Gaussian quadrature is difficult. Thus, the removal of near singularity has attracted the enthusiasm of many researchers. Many kinds of methods have been proposed for the removal of near singularity, such as the element subdivision method [9–11], semi-analytical or analytical integral method [12–15], distance transformation [16–19], PART transformation [20,21], exponential transformation [22–25], and sinh method [26–30]. Among these methods, sinh method is widely used to deal with nearly singular integrals on linear elements or in 2D BEM. We expand the sinh method to problems on thin bodies in the 3D BEM, in the integration space. Using our method, the upper and lower bounds of the polar coordinates can be obtained easily.

In our method, the distance in the denominator of the fundamental solution using the Taylor expansion by one order is designed as an approximate expansion form. We can obtain the simple and clear form of the fundamental solution and the sinh method can be introduced. In this step, the method to obtain the project point is very important. Thus, we classify the method in two cases. The Newton-Raphson (NR) method is employed to obtain the projection point. The sinh method can be directly applied if the projection point is inside the element where near singularity appears. Otherwise, another point (nearest point) is introduced. The sinh method can also be applied if the nearest point is in the element or on the element edge. The method to obtain the nearest point is as follows. First, the projection point is located by the NR method. The project point is inside the element if the projection point coincides with the nearest point. Otherwise, the minimum distance from the edge of the integration element to the source point should be confirmed to obtain the nearest point through a cubic equation. Moreover, we map the sub-triangles in a local coordinate to another local integral coordinate during the implementation of the sinh transformation. Thus, the upper and lower bounds of the pole in the polar coordinates can be obtained easily. The proposed method is validated by two numerical examples.

The contents of this paper are as follows. Section 2 provides a general form of the integrals with near singularity. Section 3 describes the distance in the local coordinate and introduces the sinh method. In Section 4, the approach in obtaining the nearest point and the process of implementing the sinh transformation are proposed. Section 5 presents two numerical examples. Section 6 presents the conclusions.

2 General form of integrals with near singularity

In this part, the general form of integrals with near singularity in 3D BEM is described. First, take 3D potential problems for examples. The well-known couple boundary integral equations (BIEs) are as follows:

$$C(Q)u(Q) = \int_\Gamma u(P)q^*(P,Q)\mathrm{d}\Gamma - \int_\Gamma q(P)u^*(P,Q)\mathrm{d}\Gamma, \tag{1a}$$

$$q_m(Q) = \int_\Gamma q(P)\frac{\partial u^*(P,Q)}{\partial s_m}\mathrm{d}\Gamma - \int_\Gamma u(P)\frac{\partial q^*(P,Q)}{\partial s_m}\mathrm{d}\Gamma, \quad m = 1,2,3. \tag{1b}$$

In Eqs. (1a) and (1b), C is the coefficient ($C=1$ for internal points and $C=1/2$ for smooth boundary points), u is the displacement, q is the flux, Q is the source point, P is the field point, s_m and x_m are the components of Q and P, respectively. Specifically, $u^*(P,Q)$ is the fundamental solution with near weak singularity, $q^*(P,Q)$ and $\partial u^*(P,Q)/\partial s_m$ are the gradients of the fundamental solution with near strong singularity, and $\partial q^*(P,Q)/\partial s_m$ is the gradient of fundamental solution with near hyper-singularity. The expression can be found in Ref. [1]. The displacement at the boundary nodes can be calculated by Eq. (1a), while the flux in the domain can be calculated by Eq. (1b). The discretize with boundary element and elements Γ_n, $n=1, 2, \ldots, N$, are represented by shape functions. Thus, the integral kernel in Eqs. (1a) and (1b) will be with near singularity if the ratio between Point Q and the edge length of Γ_n is very small. The near singularity of the integral kernel in Eqs. (1a) and (1b) is also different.

In our work, the sinh method is developed to regularize the boundary integrals with different order of singularities. We discuss details of the method in the next sections. After the boundary is discretized, the integrals in Eqs. (1a) and (1b) can be expressed clearly and generally in the following form:

$$I = \int_{\Gamma_n} \frac{f(P,Q)}{r^l}\mathrm{d}\Gamma, \; l = 1,3,5, \tag{2}$$

where I is the general form of the integral, $r = \sqrt{(s_1-x_1)^2 + (s_2-x_2)^2 + (s_3-x_3)^2}$, f is smooth, composed of shape functions and Jacobi, which can be directly calculated by Gaussian quadrature and l is the order of the distance r. The very small distance between Points Q and P compared with the size of Γ is considered only.

3 Equivalence distance in the element local coordinate and the sinh method

3.1 Equivalence form of the distance r in fundamental solution

In Fig. 1, employing Taylor expansion by one order [16–19] nearby the vertical Point P^c, which is the intersection point of the vector $\boldsymbol{n}$ and the surface element, we can obtain:

$$\begin{aligned} x_k - s_k &= x_k - x_k^c + x_k^c - s_k \\ &= \left.\frac{\partial x_k}{\partial \xi}\right|_{\substack{\xi_1=\xi_0 \\ \eta_1=\eta_0}} (\xi-\xi_0) + \left.\frac{\partial x_k}{\partial \eta}\right|_{\substack{\xi_1=\xi_0 \\ \eta_1=\eta_0}} (\eta-\eta_0) \\ &\quad + r_0 n_k(\xi_0,\eta_0) + O(\rho^2) \\ &= \rho A_k(\theta) + r_0 n_k(\xi_0,\eta_0) + O(\rho^2), \end{aligned} \tag{3}$$

where x_k^c is the component of Point P^c, ξ and η are the local coordinates, ξ_0 and η_0 is the local coordinate of the vertical point, n_k is the component of $\boldsymbol{n}$, $k=1, 2, 3$. Using polar coordinate transformation at P^c in local system, ρ is the polar, r_0 is the distance between the source Points Q and P^c, $A_k(\theta) = \left.\frac{\partial x_k}{\partial \xi}\right|_{\substack{\xi=\xi_0 \\ \eta=\eta_0}} \cos\theta + \left.\frac{\partial x_k}{\partial \eta}\right|_{\substack{\xi=\xi_0 \\ \eta=\eta_0}} \sin\theta$.

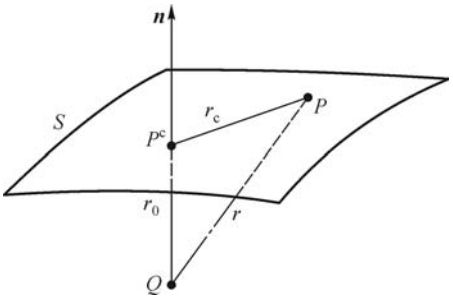

Fig. 1 Vertical distance r_0, between the source point Q and the integration element S

Employing Eq. (3), the square of the distance can be obtained by Eq. (4).

$$r^2 = (x_k - s_k)(x_k - s_k) = A_k^2(\theta)\rho^2 + r_0^2 + O(\rho^3). \tag{4}$$

Substituting Eq. (4) into Eq. (2), the form of Eq. (2) becomes:

$$\begin{aligned} I &= \int_S \frac{f(P,Q)}{r^l} \mathrm{d}S \\ &= \sum_i \int_{\theta_i}^{\theta_{i+1}} \int_{\rho_1(\theta)}^{\rho_2(\theta)} \frac{g(\rho,\theta)}{(\rho^2+\omega^2(\theta))^{l/2}} \mathrm{d}\rho\mathrm{d}\theta, \end{aligned} \tag{5}$$

where $\omega(\theta) = \dfrac{r_0}{A(\theta)}$, $A(\theta) = \sqrt{A_k(\theta)A_k(\theta)}$, and $g(\rho,\theta)$ is a smooth function. $\rho_1(\theta)$ and $\rho_2(\theta)$ are the upper and lower bounds, which need to be deduced.

3.2 Sinh method

In Refs. [19–24], the sinh transformation is introduced for the integral as follows:

$$I = \int_0^{\Theta} \int_0^{R(\theta)} \frac{rf(r\cos\theta, r\sin\theta)}{(r^2+b^2)^{\lambda}} \mathrm{d}r\mathrm{d}\theta. \tag{6}$$

Apply the sinh transformation [17–22],

$$r(s) = b\sinh(\mu_1 s - \eta_1). \tag{7}$$

Employing the following transformation, the intervals $[0,R(\theta)]$ and $[0,\Theta]$ can be mapped into $[-1,1]$, giving

$$\mu_1 = -\eta_1 = \frac{1}{2}\arcsin\frac{R(\theta)}{b} \quad \text{and} \quad \theta(\phi) = \frac{\Theta}{2}(\phi+1). \tag{8}$$

From Section 3.1 and Eq. (5), the following integral should be calculated accurately to compute nearly singular integrals directly.

$$I_i = \int_{\theta_i}^{\theta_{i+1}} \int_{\rho_1(\theta)}^{\rho_2(\theta)} \frac{g(\rho,\theta)}{(\rho^2+\omega^2(\theta))^{l/2}} \mathrm{d}\rho\mathrm{d}\theta. \tag{9}$$

$\rho_1(\theta)$ should be equal to zero, that is, the projection point should be inside the integration element to apply the original sinh transformation Eqs. (7) and (8). Otherwise, the sinh transformation cannot be used directly. Thus, we introduce the nearest point in this paper instead. The location of the nearest point is in the element or element edges. Thus, the original sinh transformation should be refined as follows:

$$r(s) = \omega(\theta)\sinh(\mu_1 s - \eta_1). \tag{10}$$

Mapping $[0,\rho_2(\theta)]$ and $[\theta_m,\theta_{m+1}]$ into $[-1,1]$ respectively gives

$$\begin{aligned} \mu_1 &= -\eta_1 = \frac{1}{2}\arcsin\frac{\rho_2(\theta)}{\omega(\theta)}, \\ \theta(\phi) &= \frac{(\theta_{m+1}-\theta_m)}{2}(\phi+1). \end{aligned} \tag{11}$$

Using Eqs. (10) and (11), the refined sinh transformation can be used directly to compute integrals with near singularity. In the next section, how to find the nearest point and implement the sinh transformation will be introduced.

4 The nearest point and the sinh transformation in local integral coordinate

4.1 Obtaining the nearest point

In Fig. 2, serendipity quadrilateral quadratic element [1] is

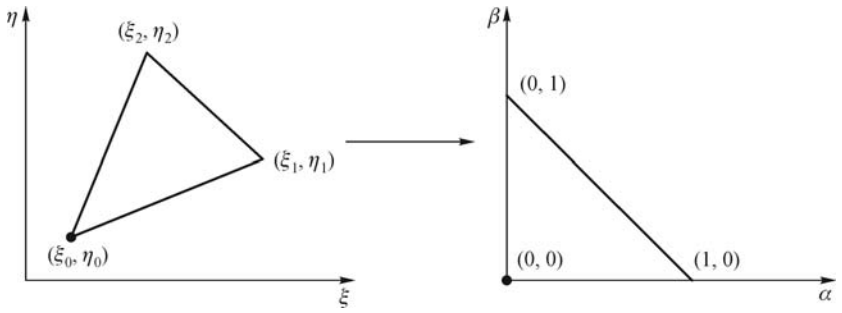

Fig. 2 Coordinate transformation from the (ξ,η) space to integration space (α,β)

taken as an example. P is the field point and P^c is the projection point. The vertical distance r from the source point Q to integration element S is represented as $|P-P^c|$. For arbitrary P on S, we have

$$x_k(\xi,\eta)=\sum_{j=1}^{8}N_j(\xi,\eta)x_k^j, \tag{12}$$

where ξ, η are the local coordinates, x_k is the coordinate components of the field point and x_k^j are the coordinate components of the element nodes, $k=1, 2, 3$. $N_j(\xi,\eta)$ is the shape function of the 8-node quadrilateral element and j is the number of shape function, $j=1, 2, \ldots, 8$.

Assume that the projection point P^c is located on the boundary element S, the local coordinates in the (ξ,η) space are (ξ_0,η_0), we have the Cartesian coordinates using the local coordinate $P^c=(x_1(\xi_0,\eta_0),x_2(\xi_0,\eta_0),x_3(\xi_0,\eta_0))$. d is the distance between the source point Q and integration element S, employing the NR method and computing $d=\|Q-P^c\|$. From the geometrical relationship in Fig. 1, we can obtain

$$\begin{cases}[x_m(\xi_0,\eta_0)-s_m]\dfrac{\partial x_m}{\partial\xi}=0\\ [x_m(\xi_0,\eta_0)-s_m]\dfrac{\partial x_m}{\partial\eta}=0\end{cases}, \tag{13}$$

where the tensor mark is used, $\dfrac{\partial x_m}{\partial\xi}=\dfrac{\partial x_m}{\partial\xi}\Big|_{\substack{\xi=\xi_0\\ \eta=\eta_0}}$, $\dfrac{\partial x_m}{\partial\eta}=\dfrac{\partial x_m}{\partial\eta}\Big|_{\substack{\xi=\xi_0\\ \eta=\eta_0}}$, and $m=1, 2, 3$.

If Q is considerably near boundary S, the distance between Q and P^c is very small. The roots (ξ_0,η_0) can be obtained using NR method. Assuming

$$\begin{aligned}f_1(\xi,\eta)&=[x_m(\xi,\eta)-s_m]\frac{\partial x_m}{\partial\xi},\\ f_2(\xi,\eta)&=[x_m(\xi,\eta)-s_m]\frac{\partial x_m}{\partial\eta},\end{aligned} \tag{14}$$

the following can be obtained:

$$F'(\xi^{(i)},\eta^{(i)})\left(\Delta\xi^{(i)},\Delta\eta^{(i)}\right)^{\mathrm{T}}=-F(\xi^{(i)},\eta^{(i)}), \tag{15}$$

$$F\left(\xi^{(i)},\eta^{(i)}\right)=\begin{bmatrix}f_1\left(\xi^{(i)},\eta^{(i)}\right)\\ f_2\left(\xi^{(i)},\eta^{(i)}\right)\end{bmatrix},$$

$$F'\left(\xi^{(i)},\eta^{(i)}\right)=\begin{bmatrix}\dfrac{\partial f_1}{\partial\xi} & \dfrac{\partial f_1}{\partial\eta}\\ \dfrac{\partial f_2}{\partial\xi} & \dfrac{\partial f_2}{\partial\eta}\end{bmatrix}_{\xi=\xi^{(i)},\eta=\eta^{(i)}},$$

$$\frac{\partial f_1}{\partial\xi}=[x_m(\xi,\eta)-y_m]\frac{\partial^2x_m}{\partial\xi^2}+\frac{\partial x_m}{\partial\xi}\frac{\partial x_m}{\partial\xi},$$

$$\frac{\partial f_2}{\partial\xi}=[x_m(\xi,\eta)-y_m]\frac{\partial^2x_m}{\partial\xi\partial\eta}+\frac{\partial x_m}{\partial\xi}\frac{\partial x_m}{\partial\eta},$$

$$\frac{\partial f_1}{\partial\eta}=[x_m(\xi,\eta)-y_m]\frac{\partial^2x_m}{\partial\xi\partial\eta}+\frac{\partial x_m}{\partial\eta}\frac{\partial x_m}{\partial\xi},$$

$$\frac{\partial f_2}{\partial\eta}=[x_m(\xi,\eta)-y_m]\frac{\partial^2x_m}{\partial\eta^2}+\frac{\partial x_m}{\partial\eta}\frac{\partial x_m}{\partial\eta}.$$

where i is the iterator, $\Delta\xi$ and $\Delta\eta$ are the increments, $\Delta\xi=\xi^{(i+1)}-\xi^{(i)}$, $\Delta\eta=\eta^{(i+1)}-\eta^{(i)}$, and T is the transpose symbol.

The effective evaluation of the location of P^c in the local coordinate of the element is important for the implementation of the proposed scheme. Picking up the initial point is crucial for NR method. In our method, we first assume that the 8-node quadrilateral element is a 4-node quadrilateral element using only the four nodes at the corners. Thus, we obtain the initial point by using the NR method on the 4-node quadrilateral element.

The position of P^c is judged. P^c is not the nearest point if the location of P^c is outside of the element where near singularity arises. The nodes of the original 8-node element

are connected and the element is treated as a curved surface element. The four edges of the element are considered and the minimum distance between Q and the four edges is determined. Thus, we can find one of the coordinates (ξ,η) in the 8-node quadrilateral element. The edge is treated as a 3-node quadratic isoparametric element and the coordinates of the edge are assumed as follows:

$$x_k(\zeta) = N_1(\zeta)x_k^1 + N_2(\zeta)x_k^2 + N_3(\zeta)x_k^3,$$

$$k = 1,\ 2,\ 3, -1 \leqslant \zeta_1 \leqslant 1, \tag{16}$$

where $N_1(\zeta)$,$N_2(\zeta)$, and $N_3(\zeta)$ are the shape functions, which are widely used in 3-node quadratic isoparametric elements. The nearest point in the ζ coordinate can be obtained by solving the following cubic equation.

$$[x_i(\zeta_0) - s_i]\frac{\partial x_i}{\partial \zeta} = 0,\ i = 1,\ 2,\ 3, \tag{17}$$

where ζ_0 is the parametric coordinate in the ζ coordinate. Thus, the parametric of the coordinates in the (ξ,η) coordinates can also be obtained.

Finally, the sub-triangle Δ_j in the local coordinate space of the element is transformed according to Δ_j. The improved sinh method can be used to regularize the integrals with near singularity. We can employ the Gaussian quadrature directly. The implementation of element subdivision can be found in Ref. [25]. The details of the processing of the numerical implementation of the sinh method in the integration space will be discussed in the next section.

4.2 Implementation of the sinh transformation in local integral coordinate

A coordinate transformation from the (ξ,η) space to the integral space (α,β) is introduced to implement sinh transformation. Figure 2 shows that the coordinate transformation as follows:

$$\begin{aligned} \xi &= (1-\alpha-\beta)\xi_0 + \alpha\xi_1 + \beta\xi_2, \\ \eta &= (1-\alpha-\beta)\eta_0 + \alpha\eta_1 + \beta\eta_2. \end{aligned} \tag{18}$$

Equation (3) can be revised using Eq. (18) as follows:

$$\begin{aligned} x_k - s_k &= x_k - x_k^{\mathrm{c}} + x_k^{\mathrm{c}} - s_k \\ &= \frac{\partial x_k}{\partial \alpha}[\alpha(\xi_1 - \xi_0) + \beta(\xi_2 - \xi_0)] \\ &\quad + \frac{\partial x_k}{\partial \beta}[\alpha(\eta_1 - \eta_0) + \beta(\eta_2 - \eta_0)] \\ &\quad + r_0 n_k(\xi_0,\eta_0) + O(\rho^2) \\ &= \rho A_k(\theta) + r_0 n_k(\xi_0,\eta_0) + O(\rho^2). \end{aligned} \tag{19}$$

In Eq. (19), $\dfrac{\partial x_k}{\partial \alpha} = \dfrac{\partial x_k}{\partial \xi}\dfrac{\partial \xi}{\partial \alpha} + \dfrac{\partial x_k}{\partial \eta}\dfrac{\partial \eta}{\partial \alpha}$, $\dfrac{\partial x_k}{\partial \beta} = \dfrac{\partial x_k}{\partial \xi}\dfrac{\partial \xi}{\partial \beta} + \dfrac{\partial x_k}{\partial \eta}\dfrac{\partial \eta}{\partial \beta}$, $\dfrac{\partial x_k}{\partial \alpha} = \left.\dfrac{\partial x_k}{\partial \alpha}\right|_{\substack{\alpha=0\\ \beta=0}}$, $\dfrac{\partial x_k}{\partial \beta} = \left.\dfrac{\partial x_k}{\partial \beta}\right|_{\substack{\alpha=0\\ \beta=0}}$.

The sinh transformation can be applied directly using the polar transformation in the integration space (α,β). For each sub-triangle Δ_j, $[\theta_1,\theta_2] = [0,\pi/2]$ and $[0,R(\theta)] = [0,\sqrt{2}/\cos(\theta-\pi/4)]$. Thus, this method can be easily integrated into the BEM codes.

5 Numerical examples

5.1 One-eighth hollow sphere

The first case considers the one-eighth hollow sphere potential problem. Two analytical solutions are imposed as the displacement boundary on all faces for the convenience of the comparison with the analytical results [11]. The two analytical solutions are as follows:

$$u(x,y,z) = x + y + z, \tag{20}$$

$$u(x,y,z) = xy + yz + zx. \tag{21}$$

This example concerns a one-eighth hollow sphere. In this example, all parameters are dimensionless. The inner radius of the eighth hollow sphere is 3.96 and the outer radius is 4.0. The wall thickness of the eighth hollow sphere is thin compared with the inner and outer radii. The near singularity of the integrals needs to be removed to analyze this problem accurately. In this example, we use the sinh method in the integration space as described in the above section. A density of 1.14 and a heat conduction of 1 are assumed. The mesh model is shown in Fig. 3, and the evaluation points are arranged in the boundary and domain. The boundary evaluation points are located in the inner and side surfaces of the parameter space [u, v], as shown in Fig. 4, where u and v belong to [0, 1]. Parameter u is from 0 to 1 and v = 0.5 in the inner and side surfaces. A total of 176 elements and 531 nodes are employed. Figures 5 to 8 show the computational results of the domain and boundary sample points.

Figure 5 shows that the computational results of the domain sample points with a linear solution by the proposed method agree well with the analytical solutions. Compared with the analytical solutions, the largest error of our method is about 0.5%. Figure 6 shows that the computational results of the boundary sample points with a linear solution by the proposed method agree well with the analytical solutions. Compared with the analytical solutions, the largest error is about 1%. Figure 7 shows that the computational results of the domain sample points with a quadratic solution by the proposed method agree well with

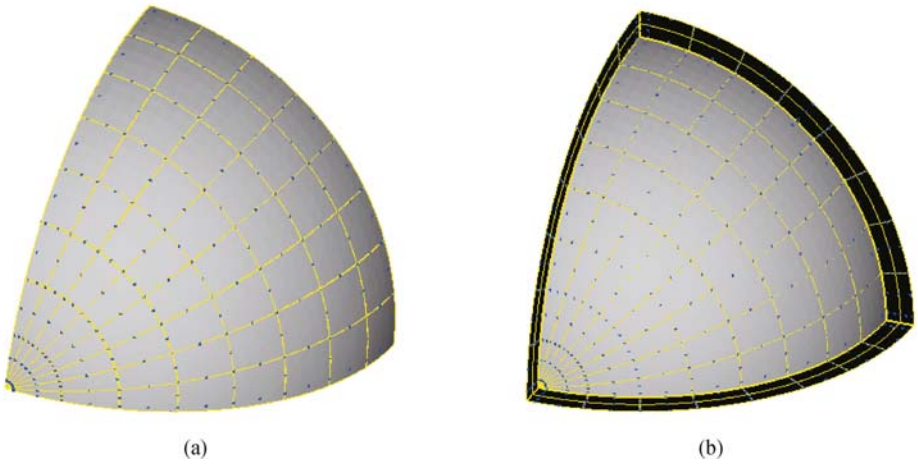

Fig. 3 Meshes of the eighth hollow sphere. (a) External view; (b) internal view

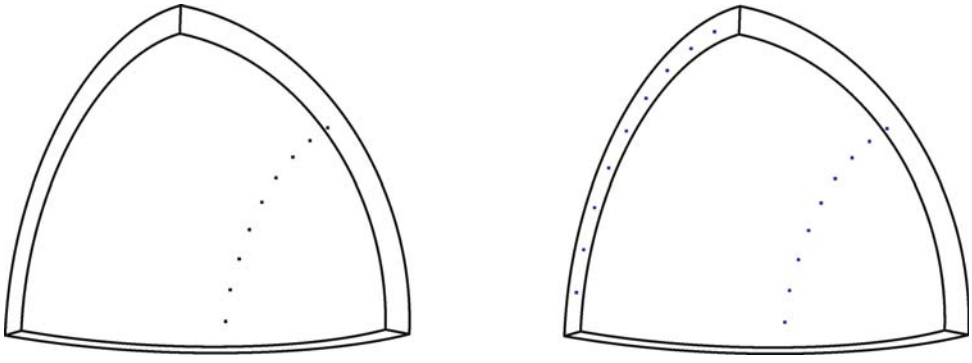

Fig. 4 Domain and boundary evaluation points of the eighth hollow sphere

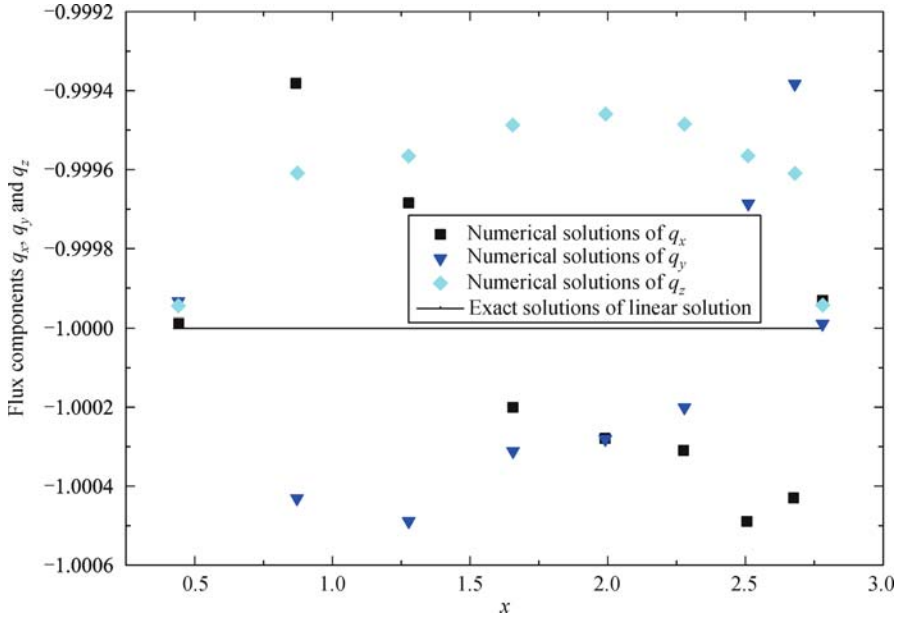

Fig. 5 Numerical solutions of domain sample points with linear solution

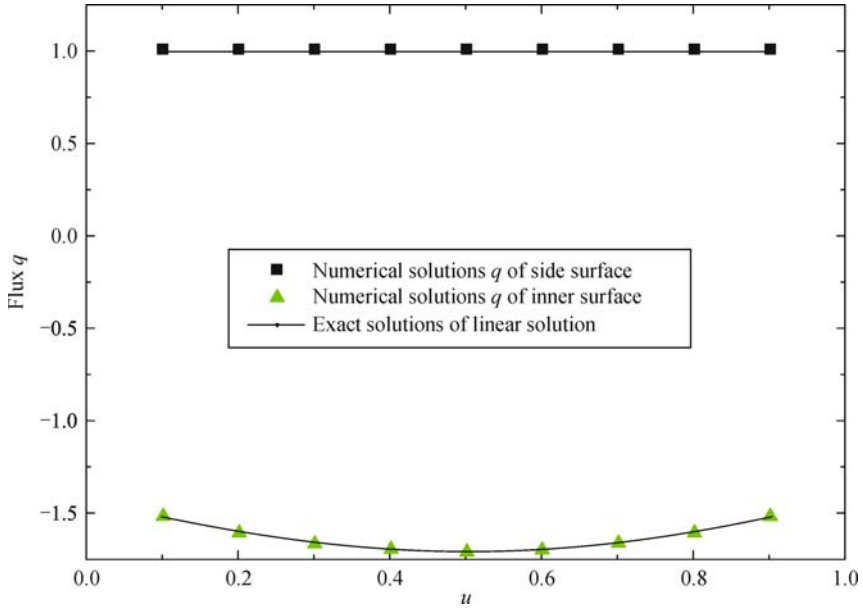

Fig. 6 Numerical solutions of boundary sample points with linear solution

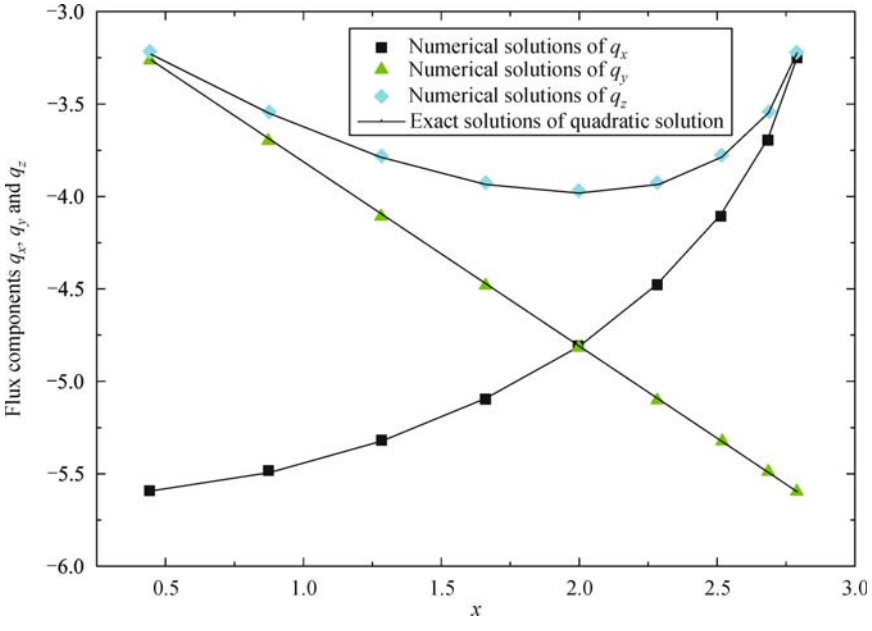

Fig. 7 Numerical solutions of domain sample points with quadratic solution

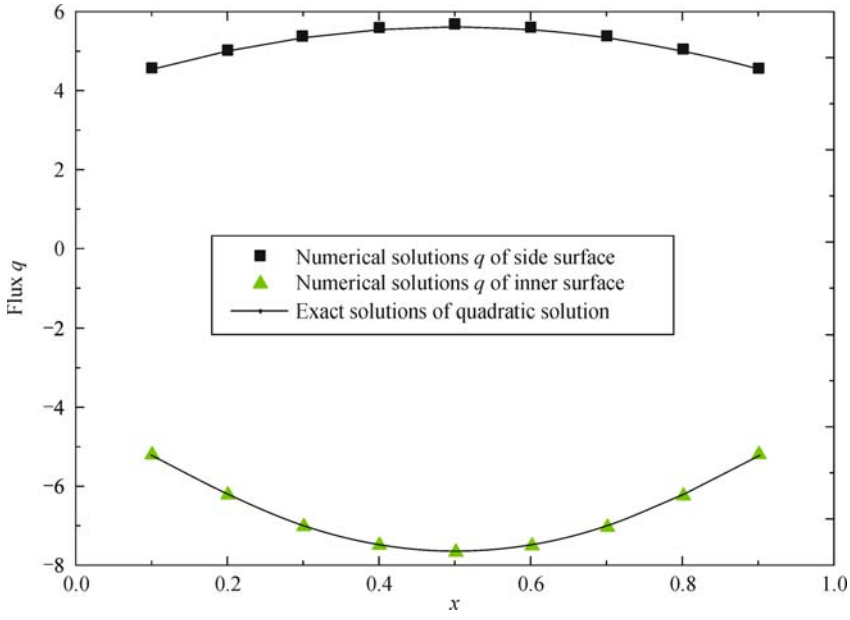

Fig. 8 Numerical solutions of boundary sample points with quadratic solution

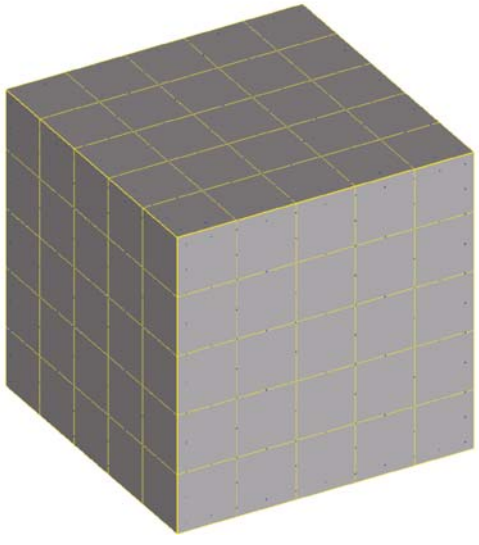

Fig. 9 Meshes of the hollow square

the analytical solutions. Compared with the analytical solutions, the largest error is about 0.3%. Figure 8 shows that the computational results of the boundary sample points with a quadratic solution by the proposed method agree well the analytical solutions. Compared with the analytical solutions, the largest error is about 0.4%.

5.2 Dirichlet problems on a hollow square

In this example, Dirichlet problems on a hollow square are computed and all parameters are dimensionless. The mesh model is illustrated in Fig. 9. The domain and boundary evaluation points are illustrated in Fig. 10. The outer edge length of the hollow square is 1 and the inner edge length is 0.99. A total of 300 8-node quadrilateral elements are used and the total number of nodes is 1152. The evaluation points are linearly distributed at the outer surface of the hollow square. Figure 9 shows that u and v represent the two directions of the surface of the hollow square. Parameter u is from 0 to 1 and $v = 0.5$ in the parameter space of the middle line. In addition, parameters u and v are from 0 to 1 in the parameter space (u, v) of the diagonal

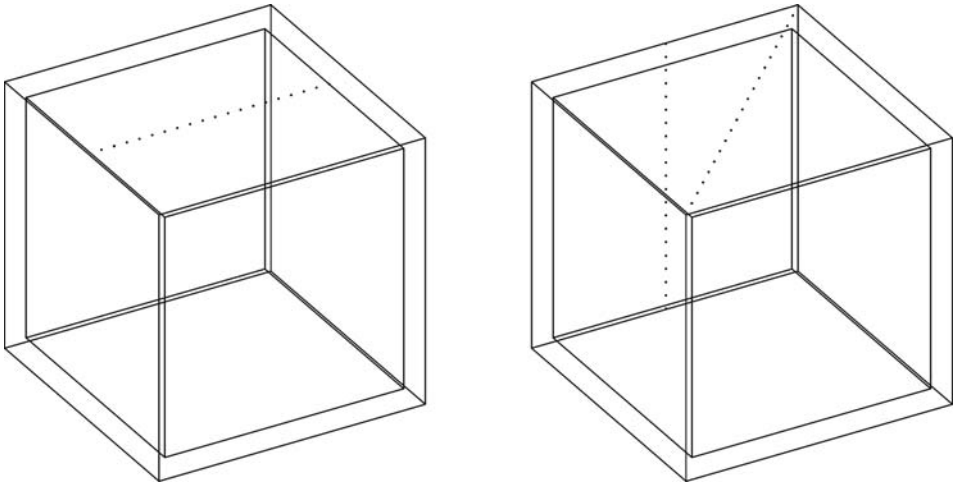

Fig. 10 Domain and boundary evaluation points of the hollow square

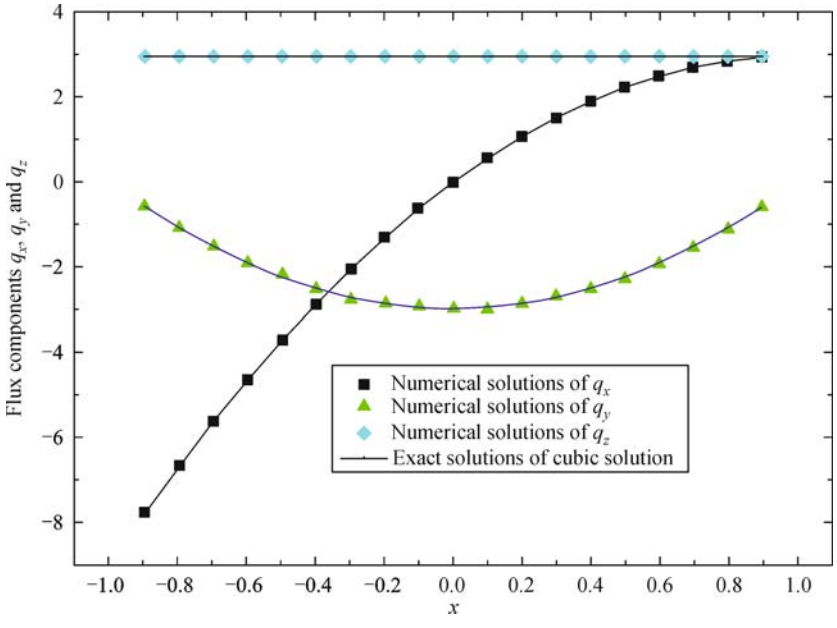

Fig. 11 Numerical solutions of domain sample points of cubic solution

line. Dirichlet conditions are added on all the faces of the hollow squares by the following cubic solution.

$$u = x^3 + y^3 + z^3 - 3yx^2 - 3xz^2 - 3zy^2. \quad (22)$$

The wall of the hollow square is thin compared with the lengths of the inner and outer edges. The near singularity of the integrals need to be removed to analyze the problems accurately. The numerical results of the domain and boundary evaluation points are illustrated in Figs. 11 and 12. Figure 11 shows that the numerical results by the proposed method agree well with the analytical solutions. Compared with the analytical solutions, the largest error is about 0.6%. Figure 12 shows that the numerical results obtained by our method agree well with the analytical solutions. Compared with the analytical solutions, the largest error is within 1%.

6 Conclusions

This work proposed a new implementation of the sinh transformation in the integration space for 3D boundary

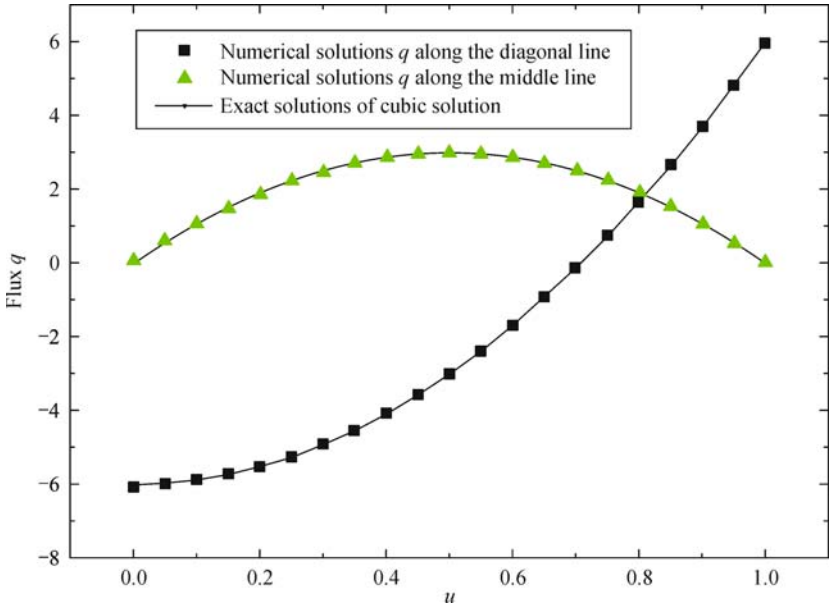

Fig. 12 Numerical solutions of boundary sample points of cubic solution

integrals with near singularity. Our goal was to improve the engineering application of BEM in CAE analysis. The sinh method was revised considering the $r_0/\sqrt{A_k^2(\theta)}$ by obtaining the equivalence distance. With the nearest point obtained by the NR method or by solving a cubic equation, the revised sinh transformation was directly performed in the integration space instead of the local coordinate space. The near singularity on the near singular subtriangles was reduced significantly by applying the revised sinh transformation and the proposed improvement approach. Our method was tested using numerical examples of potential problems on thin bodies. Results showed that our method is accurate and efficient.

Acknowledgements This work was supported in part by the National Natural Science Foundation of China (Grant Nos. 11472102 and 51476149), the Research Found for the Doctoral Program of Zhengzhou University of Light Industry, Educational Commission of Henan Province (Grant Nos. 15A460002 and 15A460037), and Xi'an Jiaotong University State Key Laboratory for Manufacturing Systems Engineering (Grant No. sklms2015012).

References

1. Liu Y. Fast Multipole Boundary Element Method: Theory and Applications in Engineering. Cambridge: Cambridge University Press, 2009
2. Feng S, Cui X, Li A. Fast and efficient analysis of transient nonlinear heat conduction problems using combined approximations (CA) method. Transfer, 2016, 97: 638–644
3. Feng S, Cui X, Chen F, et al. An edge/face-based smoothed radial point interpolation method for static analysis of structures. Engineering Analysis with Boundary Elements, 2016, 68: 1–10
4. Feng S, Cui X, Li G. Analysis of transient thermo-elastic problems using edge-based smoothed finite element method. International Journal of Thermal Sciences, 2013, 65: 127–135
5. Feng S, Cui X, Li G. Transient thermal mechanical analyses using a face-based smoothed finite element method (FS-FEM). International Journal of Thermal Sciences, 2013, 74: 95–103
6. Cui X, Liu G, Li G. A cell-based smoothed radial point interpolation method (CS-RPIM) for static and free vibration of solids. Engineering Analysis with Boundary Elements, 2010, 34(2): 144–157
7. Cui X, Feng S, Li G. A cell-based smoothed radial point interpolation method (CS-RPIM) for heat transfer analysis. Engineering Analysis with Boundary Elements, 2014, 40: 147–153
8. Cheng A H D, Cheng D T. Heritage and early history of the boundary element method. Engineering Analysis with Boundary Elements, 2005, 29(3): 268–302
9. Gao X. The radial integration method for evaluation of domain integrals with boundary-only discretization. Engineering Analysis with Boundary Elements, 2002, 26(10): 905–916
10. Gao X, Davies T G. Adaptive integration in elasto-plastic boundary element analysis. Journal of the Chinese Institute of Engineers, 2000, 23(3): 349–356
11. Zhang J, Qin X, Han X, et al. A boundary face method for potential problems in three dimensions. International Journal for Numerical Methods in Engineering, 2009, 80(3): 320–337
12. Niu Z, Wendland W, Wang X, et al. A sim-analytic algorithm for the evaluation of the nearly singular integrals in three-dimensional boundary element methods. Computer Methods in Applied Mechanics and Engineering, 2005, 31: 949–964
13. Niu Z, Zhou H. The natural boundary integral equation in potential

problems and regularization of the hypersingular integral. Computers & Structures, 2004, 82(2–3): 315–323
14. Zhou H, Niu Z, Cheng C, et al. Analytical integral algorithm in the BEM for orthotropic potential problems of thin bodies. Engineering Analysis with Boundary Elements, 2007, 31(9): 739–748
15. Zhou H, Niu Z, Cheng C, et al. Analytical integral algorithm applied to boundary layer effect and thin body effect in BEM for anisotropic potential problems. Computers & Structures, 2008, 86(15–16): 1656–1671
16. Lv J, Miao Y, Zhu H. The distance sinh transformation for the numerical evaluation of nearly singular integrals over curved surface elements. Computational Mechanics, 2014, 53(2): 359–367
17. Ma H, Kamiya N. A general algorithm for accurate computation of field variables and its derivatives near the boundary in BEM. Engineering Analysis with Boundary Elements, 2001, 25(10): 833–841
18. Ma H, Kamiya N. Distance transformation for the numerical evaluation of near singular boundary integrals with various kernels in boundary element method. Engineering Analysis with Boundary Elements, 2002, 26(4): 329–339
19. Ma H, Kamiya N. Nearly singular approximations of CPV integrals with end-and corner-singularities for the numerical solution of hypersingular boundary integral equations. Engineering Analysis with Boundary Elements, 2003, 27(6): 625–637
20. Hayami K, Matsumoto H. A numerical quadrature for nearly singular boundary element integrals. Engineering Analysis with Boundary Elements, 1994, 13(2): 143–154
21. Hayami K. Variable transformations for nearly singular integrals in the boundary element method. Publications of the Research Institute for Mathematical Sciences, 2005, 41(4): 821–842
22. Zhang Y, Gu Y, Chen J. Boundary layer effect in BEM with high order geometry elements using transformation. Computer Modeling in Engineering and Sciences, 2009, 45(3): 227–247
23. Zhang Y, Gu Y, Chen J. Boundary element analysis of the thermal behaviour in thin-coated cutting tools. Engineering Analysis with Boundary Elements, 2010, 34(9): 775–784
24. Xie G, Zhang J, Qin X, et al. New variable transformations for evaluating nearly singular integrals in 2D boundary element method. Engineering Analysis with Boundary Elements, 2011, 35 (6): 811–817
25. Xie G, Zhang J, Dong Y, et al. An improved exponential transformation for nearly singular boundary element integrals in elasticity problems. International Journal of Solids and Structures, 2014, 51(6): 1322–1329
26. Johnston P R, Elliott D. A sinh transformation for evaluating nearly singular boundary element integrals. International Journal for Numerical Methods in Engineering, 2005, 62(4): 564–578
27. Johnston B M, Johnston P R, Elliott D. A sinh transformation for evaluating two-dimensional nearly singular boundary element integrals. International Journal for Numerical Methods in Engineering, 2007, 69(7): 1460–1479
28. Gu Y, Chen W, Zhang C. Stress analysis for thin multilayered coating systems using a sinh transformed boundary element method. International Journal of Solids and Structures, 2013, 50(20–21): 3460–3471
29. Gu Y, Chen W, He X. Improved singular boundary method for elasticity problems. Computers & Structures, 2014, 135: 73–82
30. Lv J, Miao Y, Gong W, et al. The sinh transformation for curved elements using the general distance function. Computer Modeling in Engineering & Sciences, 2013, 93(2): 113–131